LIFE-TEST INVESTIGATION AND STATUS OF THE NIRISS DUAL WHEEL CRYOGENIC MECHANISM FOR JWST

Andrew S. Gibson[(1)], Ashley McColgan[(2)], Johanne C. Heald[(1)], Macso Gentilhomme[(5)], Begoña Vila[(2)], Zul Dhanji[(2)], Mike J. Anderson[(3)], Rajeev Sharma[(4)]

[(1)]*Canadian Space Agency - Space Science & Technology, 6767 Route de l'Aéroport, St-Hubert, QC, Canada, J3Y 8Y9, andrew.gibson@asc-csa.gc.ca*
[(2)] *COM DEV International, 155 Sheldon Dr., Cambridge, ON, Canada, N1R 7H6, ashley.mccolgan@comdev.ca*
[(3)]*ESTL-ESR Technology, Whittle House, 410 The Quadrant, Birchwood Park, Warrington, Cheshire, UK, WA3 6FW*
[(4)] *NASA GSFC - Electromechanical Systems Branch, MS 544, Greenbelt, MD, USA, 20771*
[(5)] *CDA Intercorp, 450 Goolsby Boulevard, Deerfield, FL, USA, 33442*

ABSTRACT

The Dual Wheel (DW) mechanism has been developed for cryogenic operation within the Fine Guidance Sensor (FGS) to fly on the James Webb Space Telescope (JWST), and has been more recently adapted to provide an updated selection of infra-red filters and grisms to enable imaging and slitless spectroscopy functions. During the flight qualification process for the mechanism, life-test goals were not met, with both wheel mechanisms achieving a significant portion of intended life, and notably the filter wheel completing a greater portion than the pupil wheel. An investigation was initiated in 2010 to determine the root cause of the life-test unit failure and to determine ways to extend mechanism life. With the reconfiguration of FGS to accommodate the Near Infrared Imager and Slitless Spectrograph (NIRISS) instrument, which evolved in parallel with the investigation, there is now a heavier reliance placed on the dual wheel, so the extension of the mechanism lifetime has become of elevated criticality to the JWST and Canadian science teams. Root causes, conclusions and status of ongoing activities for the flight hardware are described, including design enhancement and ongoing validation of the improved stepper motor gear head.

1. INTRODUCTION

FGS is provided by the Canadian Space Agency with COM DEV Ltd as prime contractor (under CSA contract 9F006-030197). The flight instrument was delivered to NASA in July of 2012. FGS is one of four JWST instruments, having the primary function to provide a redundant guiding capability (95% probability of finding a guide star anywhere in the sky). Once in fine-guide mode, the FGS will provide pointing information to a precision of < 4 milli-arcseconds at a rate of once per 64 ms for guide stars brighter than JAB ~ 19.5 magnitude. The FGS instrument also features a science module referred to as NIRISS, which enables imaging and grism spectroscopy, with a particular capability for exoplanet detection and atmospheric characterization. This functionality is provided by the DW with independently driven "Pupil" and "Filter" wheels, each containing nine elements. These elements are a combination of masks, filters and grisms to provide the various observing modes for NIRISS. Both the Filter Wheel (FW) and Pupil Wheel (PW) within the DW are driven by a stepper motor with a single-stage planetary gearhead, which combined with the pinion to ring gear (for each wheel), provides an overall gear ratio of about 91:1 (9.46 x 9.6). Position output is monitored by a resolver, geared to the ring gears at 9:1 and a variable reluctance sensor on each wheel (once per full rotation). Refer to [2] and [4] for further details of the mechanism design and instrument related requirements.

Figure 1. NIRISS Dual Wheel in the FGS instrument

2. DUAL WHEEL LIFE-TESTING

The baseline mechanism characteristics were obtained to demonstrate positioning and repeatability (precision). Each of the wheel mechanisms were tested for the specified qualification vibration, exposure to nine cryogenic cycles, survival temperature of 22K and wheel motion life testing in ambient and cryogenic conditions. Critical design requirements (torque margins, positioning, repeatability of the optic simulators and variable reluctance sensors) were tested over life. The motor drive current set point for normal operation of the DW drive electronics was 100 mA. All

Copyright © 2013 Government of Canada. The European Space Agency has been granted permission to publish and disseminate this work as part of 15th ESMATS Proceedings. All other rights are retained by the copyright owner.

torque ratios are calculated using 240 mA, which is the maximum available motor drive current (refer to [4] for relationship between torque margin and ratio). The lifetime target for the life-test unit (LTU) was based on 20% of 5.5 years on-orbit usage for both the filter wheel and the pupil wheel, with a lifetime factor of safety of 2. This factor was applied for both ground test and in-orbit operation, consistent with NASA requirements and other JWST instruments. The LTU Filter Wheel achieved an effective 67% of this original lifetime target (ambient and cryogenic rotations are combined as per Table 1). The Pupil Wheel mechanism achieved an effective 52% of this original life target. Fig.2 shows torque ratio over life (see [4] for equations relating torque ratio and torque margin). Prior to termination, the drive current settings for both had been increased to the maximum of 240mA.

The sequence of events for the life-test unit was:

26-May-10	Qualification vibration test
18-Nov-10	Start of DW life test motions
17-Dec-10	FW steps missed/not completed. Minimum current test stalled position 1-2 (100mA)
03-Jan-11	Test rack validated
11-Jan-11	FW mechanism life-test terminated (240mA)
11-Jan-11	PW mechanism testing started
01-Feb-11	PW - missed steps observed
14-Feb-11	PW current limit increased to 150mA
01-Mar-11	Analysis of motor drive phasing confirmed
04-Mar-11	PW mechanism life-test terminated (240mA)
11-Mar-11	Ambient post-life functional test
24-Mar-11	'Covers-off' inspection of ring gears

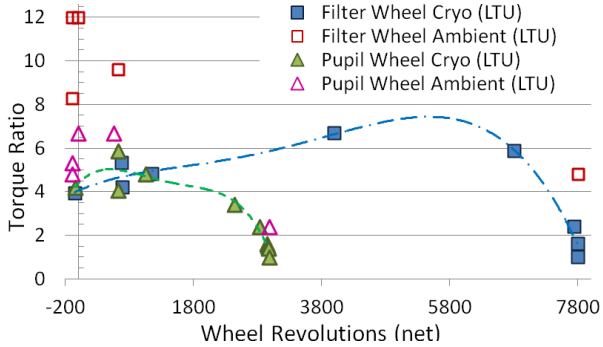

Figure 2. Torque ratio vs. Revolutions (Filter and Pupil Wheels at 35±3K) using the minimum current method

Following the life-test termination, the motors were both noted to be functional at ambient, though missing some steps. The FW showed more recovery at ambient, while the PW exhibited considerable difficulty. These points are shown in Fig.2. Sensors were all functioning nominally. Motions were limited to minimize further degradation and avoid excessive modification of evidence for the ensuing investigation. Table 1 gives a breakdown of the distribution of specific angular motions achieved at 293 and 35K versus the life test plan, with the FW achieving 64% of its cryogenic test cycles, while the PW completed 46%. Ambient life requirements for both mechanisms were exceeded.

Table 1. Dual Wheel Mechanism Life-time Status

Planned motions (incl. NASA 2X FOS)		***Lifetest Motions Planned***		***% Planned Motions Achieved****	
		293K	35K	293K	35K
Filter Wheel Motions	40°	498	10454	108%	102%
	80°	68	1404	106%	101%
	120°	926	19438	101%	83%
	160°	348	7288	101%	5%
*Net Rotations**		534	11192	**117%**	**64%**
		FW Combined		*67%*	
Pupil Wheel Motions	40°	540	5940	100%	100%
	80°	42	462	100%	100%
	120°	516	5688	105%	66%
	160°	530	5824	103%	9%
*Net Rotations**		477	5247	**117%**	**46%**
		PW Combined		*52%*	

Cryogenic columns combine ground test & mission budget
**Includes additional rotations to orient wheel during test.*

3. ROOT CAUSE INVESTIGATION

A Failure Review Board (FRB) was formed to investigate through varying levels of analyses, inspection and testing of the LTU. The team consisted of members of COM DEV, CSA, NASA-GSFC & NESC, ESTL and CDA. Early in the investigation, the FRB team established an Ishikawa-based (fishbone) exercise (Fig.4), which evolved as a guide and to track the investigation in a cause/effect manner.

The first inspection of the DW after recovery of the chamber and ambient functional checks was a 'covers-off' inspection. This included the removal of the PW baffles that covered the PW ring gears and when removed provided a clear view of the PW ring gear and the motor and resolver pinions. In addition, the Filter Wheel VR sensor cover was removed and provided some limited views of the FW gears and motor and resolver pinions. See Fig. 3 and 5 through 8.

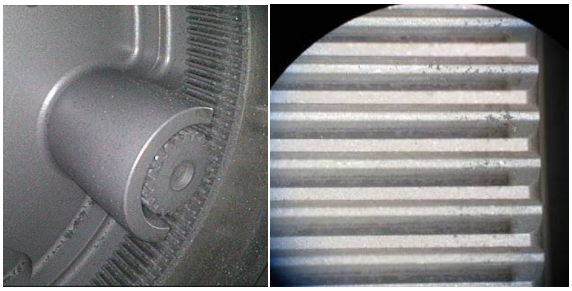

Figure 3. 'Covers off' inspection images a) wear track and related debris evident for FW ring gear, b) PW ring gear showing light wear patches

Copyright © 2013 Government of Canada. The European Space Agency has been granted permission to publish and disseminate this work as part of 15th ESMATS Proceedings. All other rights are retained by the copyright owner.

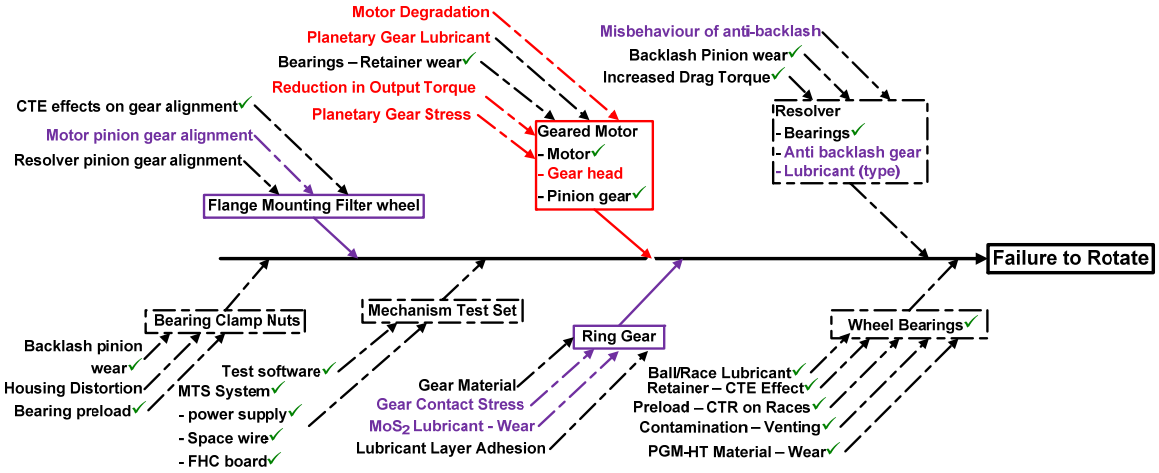

Figure 4. Ishikawa Diagram for Cause/Effect Analysis (red = factors affecting both mechanisms, purple = effect(s) exclusively observed for FW mechanism, ✓=exonerated by the investigation)

DW covers were removed, with initial observations:

- *PW ring gear to motor pinion - nominal lubricant wear.*
- *FW ring gear to motor pinion - signs of lubricant wear and localized gear tooth wear and damage.*
- *Debris was collected in vicinity of both ring gears with debris analyzed by GSFC by elemental analysis:*

  1. *Debris collected from gear and the side wall of the FWs are mixture of a dry lubricant and a PH grade stainless steel.*
  2. *Debris from the PW was mainly composed of dry lubricant. Very small amounts of iron detected, presumed to be from an iron-based alloy (Fig.5)*

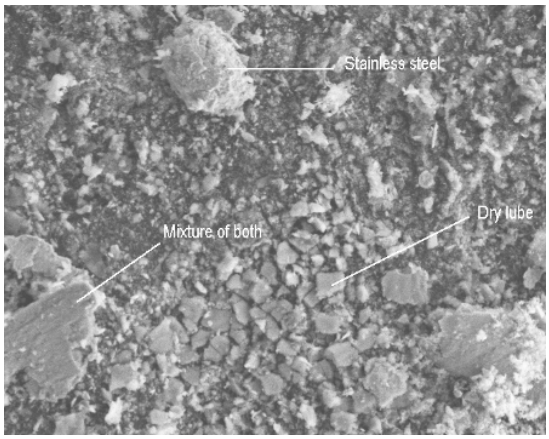

Figure 5. FW ring gear post-life debris analysis (SEM image courtesy of NASA-GSFC)

Overall, the PW inspection showed a lesser degree of wear and particulate present on gear teeth. The FW pinion also showed greater wear than the PW pinion. Resolvers showed moderate signs of pinion wear, with the greatest observed on the FW ring gear. This was expected as higher gear Hertzian contact stresses were predicted for the internally cut ring gear configuration of the FW, having notably fewer teeth on this pinion.

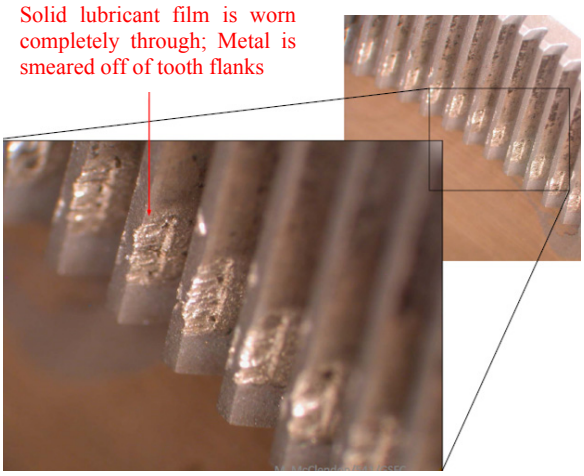

Figure 6. FW ring gear wear at motor pinion contact, with suspected anti-backlash wear feature

Detailed inspections of the gears followed with support from the Mechanisms Laboratory at NASA-GSFC:

- *FW geared motor pinion was starved of dry lubricant in some areas; in sympathy with marks on gear teeth of the ring gear, but in reasonable shape*
- *FW resolver turns, with a rough/notchy feel, while the PW resolver felt free running and smooth (ambient)*
- *MoS_2 on teeth of both resolvers- appeared different than motor pinions (traced to incorrect lubricant process)*
- *FW ring gear - MoS_2 lubricant is worn completely through, metal is smeared off of tooth flanks (refer to Fig. 6), indicating that the resolver split anti-backlash feature is a driven gear (abnormal)*

During pinion inspection, the resolver anti-backlash lubricated surface finish was observed to differ markedly from the other pinions. Traceability checks revealed that the lubricant was a mechanically applied type of MoS_2, where it had been specified as a bonded type. It was deduced that surface preparations by the

Copyright © 2013 Government of Canada. The European Space Agency has been granted permission to publish and disseminate this work as part of 15th ESMATS Proceedings. All other rights are retained by the copyright owner.

vendor were likely overly aggressive. Nonetheless, these factors were not deemed to be significant causes of the wear observed, which based on the wear pattern (Fig.6) was caused by an incorrect preload setting of the anti-backlash gear. Inspections of the PFM confirmed it to be an isolated event.

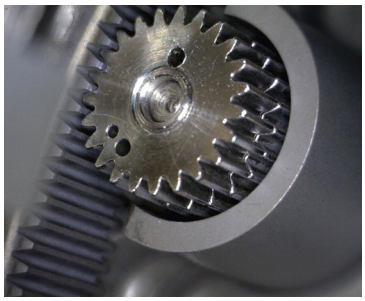

Figure 7. FW anti-backlash resolver pinion contacting internal FW ring gear

Although both bearings were found to be free-running and smooth, it was decided to inspect and perform torque traces of the bearings. The FW bearing inspections showed minor debris in areas of retainer as shown in Fig.8a. Some fine debris was present on the visible outer ring land, some of which appeared shiny. There were also some white particles, consistent with originating from the locking compound used to secure the bearing clamp rings. The PW bearings were found to be very clean as shown in Fig.8b.

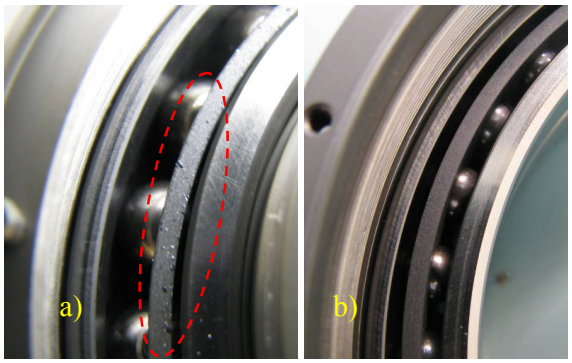

Figure 8 - Filter and pupil wheel bearing inspections a) FW (particles evident), b) pupil wheel (clean)

Detailed bearing inspections performed by ESTL noted:

- *Balls – surfaces appeared dull, with evidence of transfer from the cage, appearing as streaks on ball surfaces.*
- *Cages – only the end face and outer diameter are visible, with some particulate debris on the end face*
- *Shiny flakes present, consistent with MoS_2 worn during operation. Such debris is typically generated during running-in or the early stages of operation.*
- *Raceways – only one outer raceway, was partially visible and a ball running track was evident*
- *The ball groove is deemed normal*

Overall, the bearings did not appear to exhibit any damage or excessive wear, though it was difficult to conclude without completely disassembling the bearings. No evidence of steel debris was identified and debris was consistent with MoS_2. One Ti-alloy flake was identified; possibly produced during assembly, disassembly or removal of clamping rings. The FRB utilized the Ishikawa root cause analysis approach for systematic investigation and the "fishbone" chart was regularly updated to track and reflect exonerated items (Fig.4) and focus on contributors, postulated to have caused the DW failure.

3.1. Torque Margin Based Investigation

Having a wealth of baseline component test data which was obtained prior to assembly of the mechanism, in both ambient and cryo-test conditions, a decision was made to focus on tribological changes of key components, and commence on a program to inspect and test bearings, resolvers and motors individually. The goal was to determine the torque property changes at component level, at beginning of life, either by increasing friction or reduction of motor torque. Consideration was given to measuring the gear train friction after motor removal, but this was deemed not practical to setup, and also of less immediate utility since there was no baseline data existing. Test fixtures already existed for component level tests as described previously in [1]. It was decided to start with ambient testing of components.

A standard suite of motor tests was performed using the existing fixtures with the Vibrac test system, to measure unpowered back-drive torque, minimum current; 'pull-in' and 'pull-out' torque (@100mA excitation). Frictional torque was measured for resolvers and bearings via a strain-gauge based torque meter (Vibrac). Bearings were tested at ambient and cryogenic temperatures. There were minor spikes seen (Fig.9) possibly due to some ingress of debris, as well as some small hysteresis effects, but none of the bearing tests at ambient or cryogenic temperatures could explain a significant change in torque ratio.

The FW resolver, which felt 'notchy' on manual inspection, was sent to GSFC for a high resolution ambient torque trace (Fig.10). The test showed how sensitive a manual test can be, given that the 'notchiness' represented variations of only 0.07 N-cm peak. The PW resolver trace (Fig.11) was taken at 32K (at lower resolution), effectively exonerating this resolver given that the average and peak internal friction was minimal and test environment was representative. Two trials showed only hysteresis, detent and setup alignment effects as may be reasonably expected.

Increased noise was observed for the FW motor in back-

Copyright © 2013 Government of Canada. The European Space Agency has been granted permission to publish and disseminate this work as part of 15th ESMATS Proceedings. All other rights are retained by the copyright owner.

drive tests at ambient, though the motor was fully functional. Less evidence was found to explain changes in PW torque margin at ambient. There was little evidence of any PW geared motor degradation, prior to this motor being tested at cryogenic temperature, which was perplexing given that the PW actually experienced a more rapid degradation of torque margin.

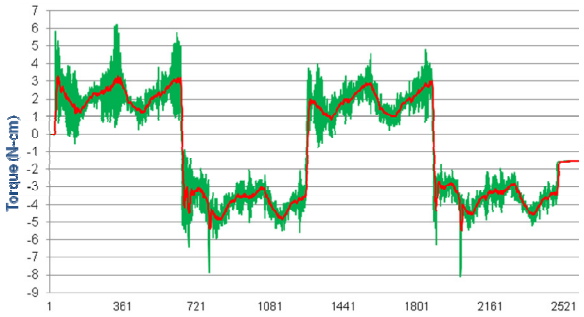

Figure 9. PW bearing post-life torque trace vs. time(s) @ 45 K, 720°, 2 cycles, 1 rpm (red = running average)

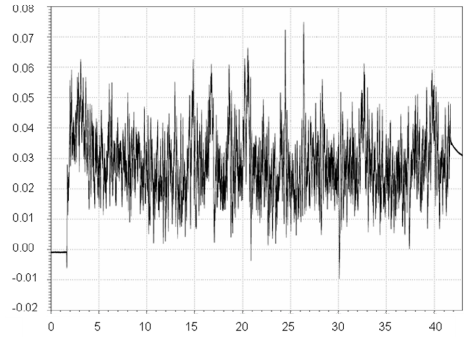

Figure 10. FW resolver ambient torque trace (N-cm) vs. Time (s) (3 revs, performed at GSFC)

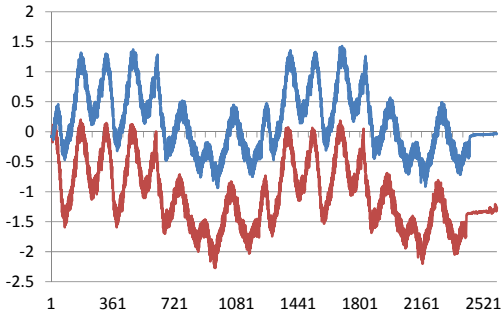

Figure 11. PW resolver @ 32K – torque trace (N-cm) vs. time(s) (2 trials shown)

The ambient trace of the PW geared motor taken at the start of the component investigation showed absolutely no concern (Fig.12), looking as though the unit had run-in nicely, with peaks seen during pre-life virtually non-existent. The average back-drive torque was almost identical to the pre-life trace. In fact, it was not until the final scheduled cryogenic test of the investigation that the PW failure would be fully explained. The motor showed inconsistent performance in pull-in and pull-out torque tests, with corresponding changes in minimum current and output torque observed. The back-drive trace showed significant and regular torque spikes (Fig.13), which exceeded 3 times the peak values seen at beginning of life as tested at 42K (less than 20 N-cm).

Figure 12. PW motor post-life ambient back-drive torque trace vs. time (s), 1 rpm

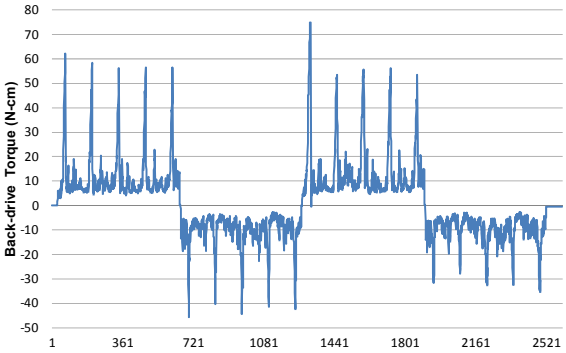

Figure 13. PW motor post-life back-drive torque trace vs. time (s) back-driven @ 32K, 1 rpm

3.2. Motor Strip-down

While the PW geared motor was under test, the PW geared motor stalled and eventually failed to rotate when commanded or manually rotated. The review board determined at this point that a full disassembly of the motor by the vendor would be required. At the CDA facility, the PW motor was disassembled. It was found that one of the 3 planet gears had become completely seized on the pin supporting the planet gear. In this condition, the PW would not rotate. This result was not entirely unexpected, as the analysis of gearhead lubrication had been identified to have low margin.

During the FW geared motor test, the motor pinion did not fail to rotate at any time, but there were signs of an increase in torque to back-drive the motor. As the only difference in the two motor designs was the output pinion, the review board authorized a disassembly and inspection of the FW motor as well. Upon inspection,

Copyright © 2013 Government of Canada. The European Space Agency has been granted permission to publish and disseminate this work as part of 15th ESMATS Proceedings. All other rights are retained by the copyright owner.

this motor also exhibited sticking of one of the planet support pins, though when rotated in the housing, the gear did rotate. Apparently, the support pin had started to free up on the housing and was now spinning in the housing seats. In this condition, the motor pinion could still rotate when commanded, but the resulting rotations would be less reliable and as debris generation and metal interference continued, a complete seizure would have resulted. When the pin was removed from the housing, the planet gear was removed from the pin. Resistance to manual rotation was felt.

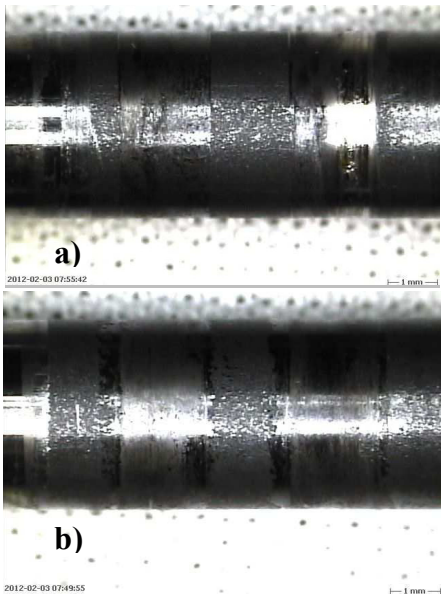

Figure 14 Wear/scoring of tungsten carbide planet pins of LTU motors (a -pupil wheel, b-filter wheel)

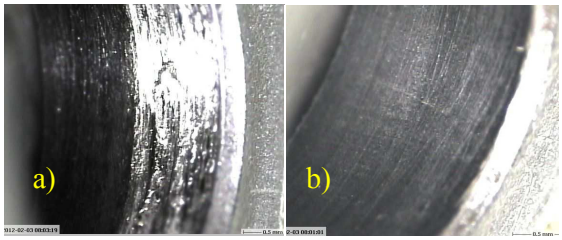

Figure 15. Wear/scoring of the planet gear - inner diameter of life-test unit (a-pupil wheel, b–filter wheel)

The cause of motor degradation was confirmed to be the wear-out of the lubricant coating of the planet support pin. It was also noted that the use of a tungsten carbide pins in this particular design had elevated contact stresses due to increase in reduced modulus of elasticity, increasing Hertzian contact stresses by approximately 20% versus steel on steel contact. It was proposed that the spikes seen in Fig.13 were related to the pin wear observed in the Figure 14a, and this was confirmed by an analysis of the planet on pin rotation frequency, being 2.26 times per rotation of the output pinion.

During end-of-life inspections of the life-test DW unit, wear marks were observed on the FW ring gear as per Fig.9, with some corresponding wear observed on the motor and resolver anti-backlash pinion. Both Table 2 and the fishbone diagram (Fig.4) summarize how the life limitation of the FW mechanism has a root cause in a combination of factors including gear misalignment contribution, while the PW failure has one root cause related to the motor gearhead. In this way, the FW drive train experienced a frictional increase due to wear, while the motor output torque reduced with time. As this wear was not present for the PW, and the motor degradations were similar, it was possible that some of the FW ring gear could have resulted from gear misalignment, in combination with an as-built issue with a reworked resolver anti-backlash gear.

Table 2. Summary of Root Cause of Degradation

Component	Filter Wheel	Pupil Wheel
Geared motor	Contributor 1	Root Cause
Resolver internal	No	No
Resolver anti-backlash gear	Contributor 2	No
Main bearing pair	No	No
Gear train friction increase due to alignment/wear	Contributor 3	No
Electronics/harness	No	No

3.3. Motor Design Improvement and Validation

The goal of the geared motor improvement initiative is to significantly improve the lifetime of the motor by addressing the life-limiting factors of the planet pin support and lubrication. A similar challenge was addressed for another JWST application, with a bushing approach applied to extend the life of a 3-stage gearhead for NIRSpec stepper motors as described in [2]. Taking note of this approach, which used a bushing to reduce stresses, and the criticality of schedule pertaining to the validation activities, a parallel approach was devised to test 2 planet support methods. The second competing approach includes a bearing-supported planet gear. Both approaches were deemed viable based on CDA's experience with similar configurations used in liquid-lubricated applications. With a larger gearhead selected, the improved motors will add a total of 0.55kg to the assembly with a larger gearhead. At present, prototypes are in test to mitigate risk, with the first life-test undergoing characterisation testing.

3.4. Motor Pinion Alignment Sensitivity Analysis and PFM Adjustment

Despite ongoing efforts to qualify a modified geared motor, it may be that existing PFM motors could still be flown with the known life-limitation. Given this

Copyright © 2013 Government of Canada. The European Space Agency has been granted permission to publish and disseminate this work as part of 15th ESMATS Proceedings. All other rights are retained by the copyright owner.

possibility, and acting on lessons learned from the life-test, it was decided to make all efforts feasible to optimise the motor pinion alignment prior to FGS shipment, and thereby maximize life by limiting ring gear wear. Changes were also intended to preclude any possibility of any tooth–to-root interference of gears. Thermal CTE analyses were re-examined for both motors and some additional margin was added to ensure that root to tip effects were precluded by increasing the spacer wire size to .010 in. for the FW and .008 in. for the PW. The assembly method for mechanism pinion to ring gear distance uses a wire spacer with the flange floating in-plane with clearance holes to allow setting this distance. The remaining degrees of freedom are the result of a tolerance stack-up. Critical interfaces include the motor mount and ring gear mounting flanges. Measurements were done in two stages: angular optical measurement of the motor mounting interface and CMM verification of critical dimensions. Optical measurements of the motor mount were made by setting a reference mirror on the rotational axis of the ring gear. With the reference co-aligned with the rotational axis, a measurement mirror was installed on the motor mount interface. The relative tip and tilt of this interface could then be measured with respect to the ring gear rotational axis with a high accuracy. CMM dimensional verification was performed to cross check.

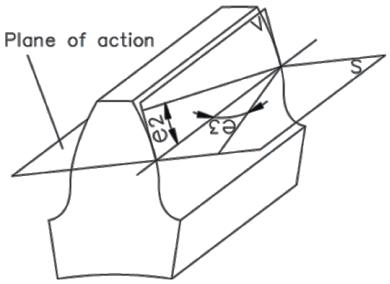

Figure 16. Gear alignment error definition [6]

As per [5], pinion-to-ring-gear misalignments can be described in 3 distinct axes. The alignment errors described in Fig.16 correspond to out-of-plane "*e2*" and in-plane "*e3*" errors with respect to the plane of action. As noted in [6], out-of-plane misalignment contribute to a rotation of the contact pattern (and stress distribution) without significantly affecting maximum stress. Contact stress is most sensitive to misalignments in the *e3* plane. PFM gear inspection photos showed evidence of a wear pattern consistent with in-plane misalignment (along tooth, *e3*). Darkened wear patches were noted toward one end of the ring gear teeth (Fig.17). Stress elevation based on misalignment was linked to stress using results presented in the ESTL handbook [7]. MoS_2 film life is estimated as inversely logarithmically proportional to contact stress. Combining the relationship for alignment vs. stress from [6] and stress vs. life [7], an estimated impact relationship of DW life vs. gear alignment was generated.

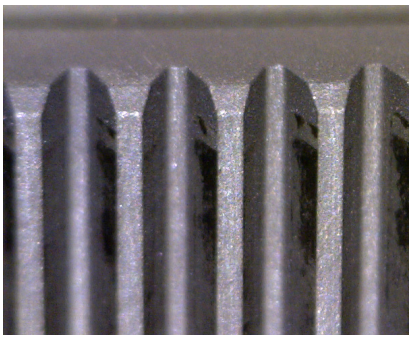

Figure 17. PFM PW ring gear wear patch arising from 'e3 type' misalignment

A linear extrapolation suggests that a 0.01º in-plane *e3* misalignment results in a 17.5% stress increase. This implies that a 0.04º misalignment results in 1.7x the design contact stress is associated with a drop in life of about 10x expected for the MoS_2 surface. This analysis confirmed the importance of verifying alignment and tracking key contributions.

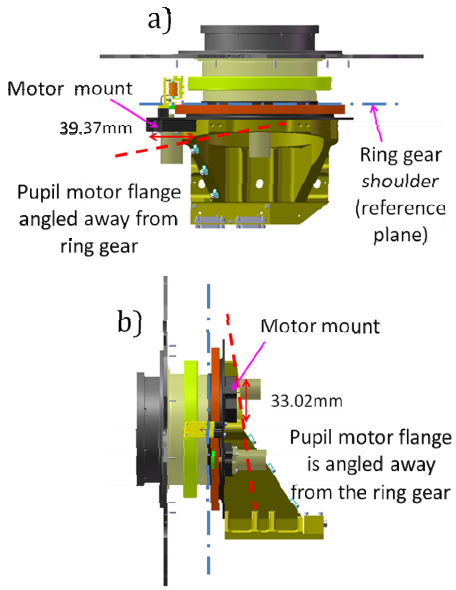

Figure 18. PW motor mount alignment observation prior to shimming a) top view and b) side view

Motors were extracted and rotational axes measured optically. The engagement and alignment modifications made were cross-checked with backlash measurements of the final configuration. PFM piece parts were found to conform to their respective drawings, however, the motor mounting flange was found to be tipped/tilted, as per Fig.18, with respect to the ring gear, consistent in direction with the findings of the optical measurement. Inspection findings were summarized:

- *Ring gears and main bearings run-out was minimal – 0.0001" to 0.0002" and measured FW and PW misalignments: 0.024º and 0.074° respectively*
- *0.0004"backlash loss due to misalignment (including*

Copyright © 2013 Government of Canada. The European Space Agency has been granted permission to publish and disseminate this work as part of 15th ESMATS Proceedings. All other rights are retained by the copyright owner.

ideal design backlash, as manufactured gears, MoS_2 lubrication, lubrication root life, angular misalignment and thermal expansion)

Motor shimming was performed to achieve final alignment within the allocated design tolerance (1.6x stress factor for misalignment, translating to 0.035º). After adjustments made to optimise the PFM motor pinion engagement, a sequence of tests were performed to re-validate the mechanism (acceptance vibration, cryo-functional and alignment check) and an ambient functional test was performed after installation into the FGS PFM instrument, purged in dry N_2.

4. STATUS OF IMPROVEMENT ACTIVITIES

The instrument, with PFM mechanisms, was delivered to NASA in July of 2012, and successfully integrated into the Instrument Science Integrated Module (ISIM) of JWST in February 2013. Three ISIM level cryo-tests are planned, with the plan to replace the DW motors (and detectors) with new motors after the 2nd cryo-test in 2014, pending demonstration of improved life via the motor life-testing in early 2014, new flight build, acceptance and delivery in 2014.

Figure 19. Improved Stepper Motor – Life-test unit

The DW motor investigation was completed in 2012. Pinion alignment was improved and backlash verification completed prior to FGS delivery. Pin loading and component stress analyses have been revised with a design review completed in June 2013. Gearhead design issues were addressed by means of 2 parallel design approaches (for risk & schedule mitigation) to reduce gearhead component wear and thereby maximize life. A development unit is in test and the first of 2 LTU's has been built with life-testing expected to be completed by May of 2014.

5. LESSONS LEARNED AND CONCLUSIONS

Following a comprehensive investigation, differences in the torque ratio evolution of the 2 drive trains through life testing, are now understood. PFM motors have been realigned for improved mechanism lifetime, with plans to swap-out the motors upon completion of new flight motor qualification. Lessons learned include:

- An early cryogenic motor level life-test with realistic loading, may have reduced programmatic impacts by establishing the life-limitation sooner
- Use of tungsten carbide pins likely increased the wear rate of the planet pin bonded MoS_2 coatings due to elevated contact stresses versus steel on steel
- Gear contact stress sensitivity - alignment parameters need to be addressed proactively and validated directly to ensure maximum lifetime. Backlash measurement was key to confirming gear spacing.
- There were significant benefits of torque monitoring through life via the simplified current method
- A measurement of gear train friction after motor removal (or via dummy rotor) could have given a quantitative assessment of the friction arising from any ring gear wear or tooth-to-root tightness.

6. ACKNOWLEDGEMENTS

The authors would like to note the contribution of Martin Leckie in leading the bulk of design, manufacture and test activities. Also of note was Mark Balzer of NASA-NESC, who provided key technical assistance during the investigation. The contributions of Peter Klimas, Sandy Beaton and Peter Cameron of COM DEV are recognized for extensive work on gear alignment sensitivity, measurement, detailed gear inspections and related analyses. Thanks to all CDA staff for their consistent cooperation and assistance throughout the investigation and design activities.

7. REFERENCES

1. Menzel, K., Jung, H.J., Schmidt, J. (2010), Development of an Actuator for Ambient to Cryo Application, *Proceedings of 40th NASA AMS*, NASA/CP-2010-216272, pp389
2. Leckie M., Ahmad Z., (2010) Development and Acceptance Testing of the Dual Wheel Mechanism for the Tunable Filter Imager Cryogenic Instrument on the JWST, *40th AMS Proceedings*, **NASA/CP-2010-216272**, pp.401
3. Leckie, M., (2010) Design and Development of the Dual Wheel and Focus Mechanism Subsystems for the Fine Guidance Sensor Cryogenic Instrument on JWST, *Proceedings of CASI-Astro*
4. Gibson, A.S., McColgan, A., Heald, J.C., Harpell, E., Anderson, M.J., Sharma, R. (2013) Overview of Design and Validation of the Fine Guidance Sensor Mechanisms for JWST, to be released *Proceedings of 15th ESMATS*
5. Shuting, Li (2007) Effects of machining errors, assembly errors and tooth modifications on loading capacity, load-sharing ratio and transmission error of a pair of spur gears, *Mechanism and Machine Theory, **42***, pp698-726
6. Miyoshi, K. (1999), Considerations in vacuum tribology, *Tribology International, **32***, pp605-616
7. *ESTL Space Tribology Handbook*, 5th Edition (2013), ESR Technology Limited section 4.2.3

Copyright © 2013 Government of Canada. The European Space Agency has been granted permission to publish and disseminate this work as part of 15th ESMATS Proceedings. All other rights are retained by the copyright owner.